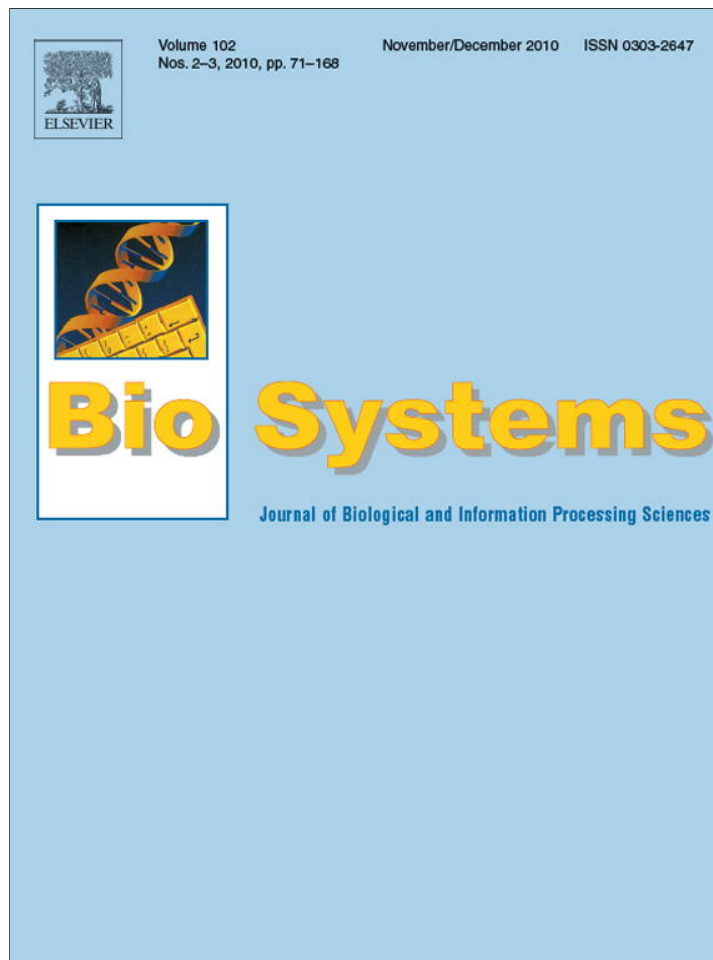


Provided for non-commercial research and education use.
Not for reproduction, distribution or commercial use.



This article appeared in a journal published by Elsevier. The attached copy is furnished to the author for internal non-commercial research and education use, including for instruction at the authors institution and sharing with colleagues.

Other uses, including reproduction and distribution, or selling or licensing copies, or posting to personal, institutional or third party websites are prohibited.

In most cases authors are permitted to post their version of the article (e.g. in Word or Tex form) to their personal website or institutional repository. Authors requiring further information regarding Elsevier's archiving and manuscript policies are encouraged to visit:

<http://www.elsevier.com/copyright>



Contents lists available at ScienceDirect

BioSystems

journal homepage: www.elsevier.com/locate/biosystems

A hierarchical approach to model parameter optimization for developmental systems

Tim Hohm^{a,b,c,*}, Eckart Zitzler^a

^a Computer Engineering and Networks Laboratory, ETH Zurich, 8092 Zurich, Switzerland

^b Department of Medical Genetics, University of Lausanne, 1005 Lausanne, Switzerland

^c Swiss Institute of Bioinformatics, Lausanne, Switzerland

ARTICLE INFO

Article history:

Received 7 December 2009

Received in revised form 21 April 2010

Accepted 5 September 2010

Keywords:

Parameter estimation

Gene regulatory Network models

Evolutionary Algorithms

Hierarchical problem decomposition

ABSTRACT

In the context of Systems Biology, computer simulations of gene regulatory networks provide a powerful tool to validate hypotheses and to explore possible system behaviors. Nevertheless, modeling a system poses some challenges of its own: especially the step of model calibration is often difficult due to insufficient data. For example when considering developmental systems, mostly qualitative data describing the developmental trajectory is available while common calibration techniques rely on high-resolution quantitative data.

Focusing on the calibration of differential equation models for developmental systems, this study investigates different approaches to utilize the available data to overcome these difficulties. More specifically, the fact that developmental processes are hierarchically organized is exploited to increase convergence rates of the calibration process as well as to save computation time.

Using a gene regulatory network model for stem cell homeostasis in *Arabidopsis thaliana* the performance of the different investigated approaches is evaluated, documenting considerable gains provided by the proposed hierarchical approach.

© 2010 Elsevier Ireland Ltd. All rights reserved.

1. Background

Mathematical modeling is one of the key tools assisting researchers when studying gene regulatory networks; it not only helps to visualize complex interactions, but in particular allows to validate hypothesis concerning system structure and dynamics *in silico* before actual experiments are carried out (Amonlirdviman et al., 2005; Bouyer et al., 2008; Geier et al., 2008; Jönsson et al., 2005; Nakamasu et al., 2009; von Dassow et al., 2000; Yamaguchi et al., 2007). With regard to developmental systems, a common question in this context is how stable patterns are established via the underlying genetic regulatory interactions where pattern refers to a spatio-temporal gene expression profile (see Fig. 1). As corresponding models, commonly differential equation formalisms are chosen since they provide the necessary level of detail and can often be derived from known reactions in a straight forward manner (Mjolsness et al., 1991; Murray, 2003; Savageau, 1979; Voit, 2000); furthermore, simulation remains computationally tractable.

Before such models can be used, model parameters like various reaction rates and kinetic constants need to be calibrated using experimental data. However, data generation for this type of systems remains difficult even when considering recent advances in experimental techniques. In an ideal case, detailed quantitative data concerning both system dimensions time and space would be available. In practice though, available data concerning interactions (Clark et al., 1997; Fletcher et al., 1999; Kondo et al., 2006; Müller et al., 2008, 2006) and patterning (Bleckmann and Simon, 2009; Gordon et al., 2007; Laux et al., 1996; Reinhardt et al., 2003) are usually of qualitative nature, cf. Fig. 1. Due to this fact, well established methods for parameter inference, e.g., Mendes and Kell (1998) and Moles et al. (2003), are not applicable and alternative methods for model calibration are required.

One approach is to analytically solve the differential equations and thereby calibrate the model behavior with respect to experimental data consisting of qualitatively defined stable tissue patterns (Koch and Meinhardt, 1994; Murray, 2003; Strogatz, 2000). Since both the spatial component and non-linear interactions often render this approach infeasible already for mid-sized systems, another strategy is to calibrate model parameters by hand guided by analytical results for comparable systems (Hohm et al., 2010; Jönsson et al., 2005; Yamaguchi et al., 2007). Here, simulated tissue patterning is compared visually to experimental data. Nevertheless, when thinking about testing of various hypothe-

* Corresponding author at: Department of Medical Genetics, University of Lausanne, Rue de Bugnon 27, 1005 Lausanne, Switzerland.

E-mail addresses: tim.hohm@unil.ch (T. Hohm), eckart.zitzler@tik.ee.ethz.ch (E. Zitzler).

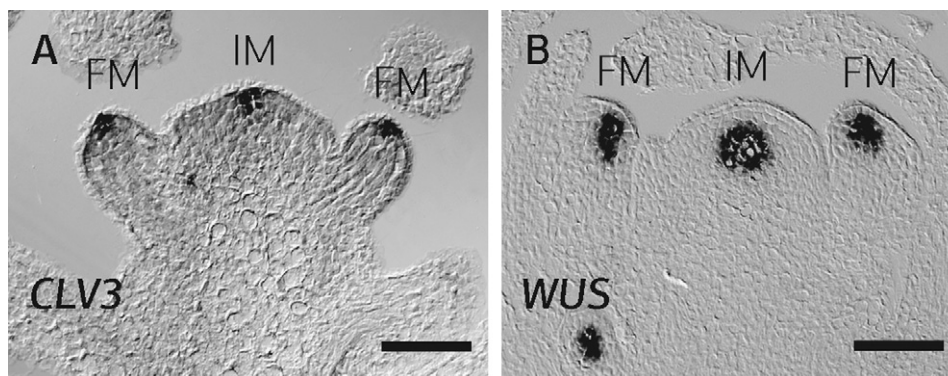


Fig. 1. Expression patterns of *CLAVATA3* (*CLV3*) and *WUSCHEL* (*WUS*) in the shoot apical meristems (SAMs) of (A) *Capsella rubella* and (B) *Arabidopsis thaliana*. IM: inflorescence meristem. FM: floral meristem. Scale = 50 μm (RNA in situ hybridizations provided by Ralf Müller, IMPS, The University of Edinburgh). Note that *in vivo*, *CLV3* expression is used as a marker for stem cell identity and *WUS* expression indicates cells belonging to the organizing center (OC).

ses, parameter calibration by hand becomes too laborious. Instead, automated optimization strategies, especially search heuristics, can be used in combination with corresponding objective functions quantifying the degree of similarity between model and data (Hohm and Zitzler, 2007, 2009a,b,c; Raffard et al., 2006; von Dassow et al., 2000); but even such search algorithms do have difficulties in finding appropriate parameters due to the model complexity and the fuzziness of the optimization goal.

In this paper, we aim at improving parameter calibration on models for developmental systems in order to make more complex models feasible. The idea is to make use of further information on the developmental trajectory and to translate this information into a hierarchical optimization procedure. More specifically, we propose to exploit the fact that developmental systems run through a series of intermediate states where each state involves only parts or loosely connected subsystems of the complete system in question, e.g., gap genes, pair rule genes, or segment polarity genes in *Drosophila* development (von Dassow et al., 2000). Knowledge about these different stages can be used to decompose the optimization task into a set of subtasks that can be tackled in a hierarchical fashion: the smallest task involving only a few model parameters is solved first, afterwards the results are used to solve the second subtask, and so forth. At each level, further model parameters are included in the optimization process until the actual, full model parameter estimation problem is addressed.

In the following, we investigate the hypotheses that such a decomposition (i) improves the convergence of search heuristics for parameter optimization and (ii) results in savings in necessary computational cost (simulations of subsystems are computationally cheaper). As test system, a differential equation model for maintenance of the patterning in the shoot apical meristem (SAM) of *Arabidopsis thaliana* is used (Hohm et al., 2010).

2. Model system background

To evaluate the possible impact of considering information on the developmental trajectory of a system during the parameter calibration process of respective models, the proposed techniques are tested on a partial differential equation model describing autonomous SAM maintenance in *A. thaliana*. Model details are presented in (Hohm et al., 2010) and only a brief review on the underlying processes is given here.

2.1. System structure

The SAM harbors a stem cell domain (SCD) located at the apical tip of the meristem (see Fig. 1A) providing the plant with a life-long supply of undifferentiated cells necessary for aerial growth and the

formation of new organs. Maintenance of the SCD relies on signals from a set of cells located underneath the SCD in the deeper cell layers, the organizing center (OC, see Fig. 1B). Communication and thereby regulation between these two domains consists of a signaling pathway originating from the SCD with its cells secreting the peptide *CLV3* (Brand et al., 2000; Fletcher et al., 1999; Kondo et al., 2006) that interacts with receptor systems expressed around the OC (Clark et al., 1997; Jeong et al., 1999; Müller et al., 2008; Ogawa et al., 2008). This signaling pathway represses expression of a homeodomain transcription factor *WUS* in the OC. *WUS* in turn acts non-cellautonomously promoting stem cell fate in the meristem tip (Groß-Hardt et al., 2002; Laux et al., 1996; Mayer et al., 1998), probably via *ARABIDOPSIS RESPONSE REGULATOR* genes that are involved in cytokinin signaling (Leibfried et al., 2005). Thereby, SCD and OC are part of a feedback loop (see Fig. 2A) that is supposed to allow for maintenance of both domains; this feedback loop is implemented in a differential equation model consisting of the following five species:

- [*WUS*]: The gene expression level or gene product concentration of the transcription factor *WUS*. Since *WUS* is a marker for OC cells that remains locally, it replaces OC identity in this model.
- [*facX*]: A factor inducing *WUS* expression while staying under negative feedback control by *WUS* through active degradation or consumption during *WUS* expression.
- [*WUS_{sig}*]: A diffusible signaling component transmitting *WUS* activity from the OC to the spatially disjunct SCD.
- [*st*]: A continuous variable representing stem cell identity.
- [*CLV3*]: The gene expression level or gene product concentration of *CLV3*, substituting *CLAVATA* signaling from SCD to OC. *In vivo*, *CLV3* expression commonly is used as a marker for stem cell identity but since it is diffusible, here stem cell identity ([*st*]) and *CLV3* expression are decoupled.

In addition to these five species and their interactions, the spatial component of the SAM plays a crucial role in order to allow for the emergence of spatially disjunct domains. In this study a simple one dimensional system consisting of 10 cells is considered (see Fig. 2C). It represents a simplified topology compared to the two dimensional spatial domain proposed in Hohm et al. (2010). This simplification allows to cut down computational costs considerably while retaining the capabilities of the system to form both functional domains. Thereby, each of the cells contains the same regulatory network and cell communication is implemented by diffusion processes between neighboring cells. The model structure including the conversion step from model hypothesis to partial differential equation representation is sketched in Fig. 2.

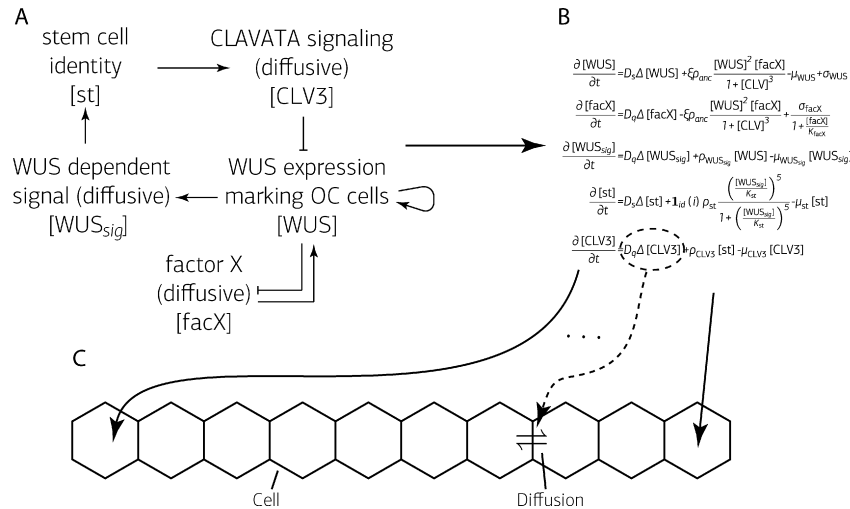


Fig. 2. Problem structure containing the assumed gene regulative network underlying stem cell homeostasis in SAMs of *A. thaliana* (A), the resulting model that is executed in each cell (B), and the considered one-dimensional spatial domain consisting of 10 cells (C). Explanations of the model equations shown in (B) can be found in Appendix A.

2.2. System dynamics

The development of systems like the SAM in *A. thaliana* can be decomposed into a series of states these systems run through. For the SAM, such a decomposition into transient states looks as follows: the structure of a wild type SAM can be described as pattern consisting of two spatially confined domains, SCD and OC (see Fig. 1). During SAM de novo assembly, first cells expressing *WUS* become visible, thereby indicating formation of an OC. Initiated by *WUS*, stem cell identity is initiated documented by the onset of *CLV3* expression (Gordon et al., 2007; Stahl and Simon, 2005). More specifically, the development of a SAM is decomposed into the following three stages:

- Emergence of an OC
- Formation of a corresponding SCD. From a modeling perspective the formation of the SCD can be further decomposed: although hierarchically structured, SAM regulation includes feedback of *CLV3* on *WUS* expression, therefore introducing a circular component to SAM development. In order to identify suitable model parameter settings, it is helpful to further disrupt this cycle by introducing an artificial intermediate step given as next item.
- A stage where the feedback of *CLV3* on *WUS* is ignored.

These three different stages result in the corresponding target patterns with respect to the model entities $[WUS]$, $[st]$, and $[CLV3]$ shown in Fig. 3. For the first stage the target pattern captures the formation of a spatially confined OC at a random location

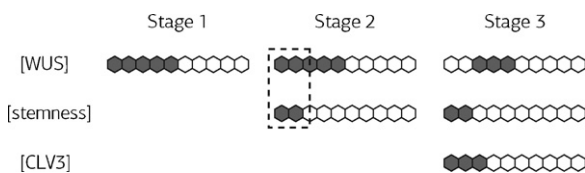


Fig. 3. Patterning of the SAM used during parameter calibration for different stages with respect to the species $[WUS]$, $[st]$, and $[CLV3]$ for a one-dimensional system. Dark hexagons indicate cells showing expression of the respective species during a certain stage while empty cells show no expression. Note that during stage 2 both OC and SCD overlap due to the neglected negative feedback of *CLV3* on *WUS* expression (cells in the dashed rectangle).

in the modeled domain. Emergence of this domain only depends on a subsystem of the used model encompassing the model entities $\{[WUS], [facX]\}$. The patterning for the second stage, on top of an OC, captures the emergence of a spatially confined SCD. Since for the second stage only $\{[WUS], [facX], [WUS_{sig}], [st]\}$ are considered and the negative feedback between SCD and OC via *CLV3* signaling is neglected, there are no constraints imposed on their relative arrangement making it most likely that both domains overlap: the negative feedback repelling both domains is missing and the promoting influence of the OC on SCD is strongest at the location of the OC. Then, for stage three the steady state patterning of a wild type meristem is used. In this pattern, both functional domains from stage two are still present, this time focusing on their relative arrangement: juxtaposition of both domains and a stable feedback between both with respect to promoting (*WUS* signaling) and inhibiting (*CLV3* signaling) influences. For this stage, all entities need to be considered.

3. Approach

The aim of model calibration is to identify a parameter setting in the model parameter space that minimizes the deviation between model output and available data. For the real-valued parameter space $X \subseteq \mathbb{R}^n$ considered for the example system SAM in *A. thaliana* such a parameter setting is described by the following expression:

$$\operatorname{argmin}_{x \in X} f(x), \tag{1}$$

where $f(x)$ quantifies the model fit by measuring the degree of dissimilarity between experimental data and model. Identifying such a parameter setting poses two different questions: (i) How can a model output be compared to available experimental data to make best use of the available information, and (ii) what optimization method can be used to identify such a setting—two aspects that are covered in the following.

3.1. Optimization model

Investigating developmental processes like growth of a plant, one observes that they take place in continuous time and involve changes in expression of a multitude of genes, ultimately responsible for the observed phenotype. Thereby, expression is pinpointed

based on concentrations of transcribed RNA or gene products, again living in a continuous scale. Still, states of such systems are commonly described involving discretizations: instead of the developmental trajectory, a certain time point is considered that often marks an equilibrium state, and concentrations are reduced to levels like high and low. Here, especially the restriction to a single point in time results in a loss of information concerning the development. Therefore, the calibration approach proposed here is designed to allow the incorporation of information on the developmental trajectory in form of a set of different system states that are considered during the calibration process.

3.1.1. Entity discretization

Since the focus of this study is on the incorporation of additional information with respect to time, the expression patterns for considered points in time are represented in a simple form using qualitative masks p . These masks can be generated for different entities and for different points in time. In order to reduce continuous concentrations to discrete, qualitative values, thresholding is used. In case of the example system SAM and the chosen level of detail it encompasses the five model entities $ent \in \{[WUS], [facX], [WUS_{sig}], [st], [CLV3]\}$. This results in patterns $p_{ent} = \{on, off\}^{|T|}$ (with T being the set of modeled cells of cardinality $|T|$). Masks p_{ent}^{sim} deduced from model simulations can then get compared to masks p_{ent}^{tar} deduced from experimentally determined expression patterns by counting differences in gene expression states between the two on a per entity and cell basis. In case of the example system SAM, p_{ent}^{tar} consists of three masks (see Fig. 3), one for each of the entities $[WUS]$, $[st]$, and $[CLV3]$. For model calibration these masks are used to define three difference functions $h_{[WUS]}^3$, $h_{[st]}^3$, and $h_{[CLV3]}^3$ that are instantiations of the following equation:

$$h_{ent}^{pt}(p_{ent}^{sim}, p_{ent}^{tar}) = \sum_{p_{ent,i}^{sim} \neq p_{ent,i}^{tar}} 1, \quad \text{for } 1 \leq i \leq |T|. \quad (2)$$

Here, pt refers to the point in time the respective mask belongs to and $pt=3$ marks the final stable pattern. Using the run index i , $h_{ent}^{pt}(p_{ent}^{sim}, p_{ent}^{tar})$ thereby sums over all cells where the simulated patterns show a different expression state than the experimentally determined patterns. This functions h then replaces the rather generic function f in Eq. (1).

3.1.2. Time discretization

Adding further time information might provide useful information for the quantification of differences between simulations and experiments. Here, the fact that developmental processes are often organized hierarchical and in effect run through a series of known transient states can be exploited.

As described in Section 2.2, the development of a SAM in *A. thaliana* can be decomposed into at least three different stages. Considering the transient stages and corresponding models (see Appendix A) in addition to the final system state adds further difference functions, complementing the difference functions $h_{[WUS]}^3$, $h_{[st]}^3$, and $h_{[CLV3]}^3$ that already have been introduced: (i) for the first stage, $h_{[WUS]}^1$ evaluating the fit of an emerging OC, and (ii) for the second stage, $h_{[WUS]}^2$ and $h_{[st]}^2$ measuring the fit of developing OC and SCD are added.

The simplest way to incorporate these stages is to always simulate all stages simultaneously. While such an approach in principle should have a maximum of information available in each stage, simulating all stages during every evaluation of a parameter setting introduces considerable overhead in terms of computation time. To avoid this overhead, it makes sense to consider the different stages in a sequential manner, an approach that is inspired by strategies for multilevel optimization (Horst et al., 1995; Migdalas

et al., 1997). Thereby, for every evaluation of a parameter setting only one modeled stage needs to be simulated. In addition, the fact that stages are ordered in a hierarchical manner can be exploited: later stages contain the subsystems and thereby already calibrated parameters from early stages and it could be possible to transfer further information between the optimization processes for consecutive stages, e.g., dependencies between involved parameters or general information on problem structure. In consequence, the problem of calibrating the model with respect to the final stage is decomposed in smaller subproblems, the sum of which could be easier to optimize than the original problem like in dynamic programming approaches.

3.2. Optimization method

Repeating the formulation for the task of model calibration given in Eq. 2, it is defined by identifying a parameter setting $x \in X$ that minimizes the difference between model output p_{ent}^{sim} and experimentally determined qualitatively defined patterning p_{ent}^{tar} for different system entities ent . The match between simulation and experimental data is quantified by functions h_{ent}^{pt} . In this context, such a parameter setting is formally described by the following expression:

$$\operatorname{argmin}_{x \in X} \{h_{ent}^{pt}(p_{ent}^{sim}, p_{ent}^{tar})\}, \quad (3)$$

for all considered points in time pt and system entities ent . Here, $X \subseteq \mathbb{R}^n$ is the n dimensional model parameter space of real numbers.

For this minimization problem, an evolution strategy is used (for a short review see Foster (2001)). Evolution strategies belong to the class of randomized optimization algorithms designed for real-valued optimization like the parameter spaces $X \subseteq \mathbb{R}^n$ considered for differential equation models in developmental biology.

In short, evolution strategies map principles of Darwinian evolution to form an optimization cycle (see Fig. 4): beginning with an initial guess on an appropriate search distribution p_X on the considered search space X (here the model parameter space) the search space is sampled λ_{SO} times and the samples x_i with $1 \leq \lambda_{SO}$ are evaluated using an objective or fitness function h (here the function quantifying the dissimilarity between model output and experimentally determined tissue patterning). Based on their respective objective or fitness scores, a subset of the λ_{SO} so called offspring vectors is selected to update the search distribution p_X . These steps are then repeated until a certain stopping criterion is met. Stopping criteria that are commonly used are, e.g., a bound on the number of objective function evaluations or a fitness threshold which once exceeded by one of the sample vectors terminates the optimization process. As search distribution, commonly normal distributions $N(m, s^2C)$ are used, with distribution mean m , a covariance matrix C , and a scaling factor s .

One of the most successful evolution strategies is the Covariance Matrix Adaption Evolution Strategy (CMA-ES) designed by Hansen and Ostermeier (2001). In each iteration of its optimization cycle it uses information on the selected x_i to infer dependencies between the different dimensions of X . Thereby, it adapts the shape of C . In addition, the scaling factor s is updated. The offspring are drawn according to:

$$x_i \sim m + sN(0, C). \quad (4)$$

Both, C and s are updated in such a way that the likelihood of sampling a point x^* that is better in terms of the fitness function than the previously drawn samples is increasing.

The CMA-ES shows a set of invariance properties that in effect make it a robust optimization method: (i) since the selection of the λ_{SO} offspring during each cycle or generation is done using a ranking of the sampled points x_i with respect to h , CMA-ES is invariant to

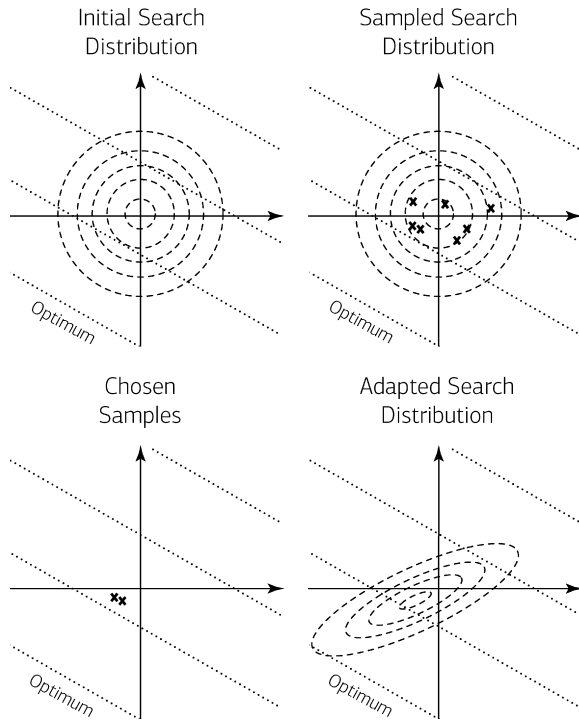


Fig. 4. Iterative optimization cycle of the Covariance Matrix Adaption Evolution Strategy (CMA-ES), documenting the adaption of a sample distribution in order to increase the probability of sampling a setting solving the considered optimization task. During this process, first the initial sample distribution is sampled; from the samples, the best candidates in terms of the objective are selected; using the selected samples, the search distribution is adapted. These steps form a cycle that is repeated until a stopping criterion is met. In the figure, the dotted lines are lines representing equal objective values and the optimum of the sketched problem is located in the bottom left corner. The dashed lines represent lines of equal probability density to sample a setting for the considered sample distributions.

order preserving transformations on h ; (ii) adaption of C is capable of inferring rotations with respect to search space axes, resulting in an invariance to rotations; (iii) adaption of s allows for some invariance to overall scaling of the parameter space, given that initial C and s are chosen appropriately. In combination, these properties make CMA-ES a search heuristic that has proven its value in a range of real valued optimization tasks (Auger and Hansen, 2005; Hohm and Zitzler, 2007, 2009b; Moles et al., 2003; Quast et al., 2005).

In the described form the CMA-ES is specialized to deal with optimization tasks where only a single objective is considered. On the other hand, in the context of model calibration often a set of objectives has to be considered, e.g., differences between simulated patterning and experimentally determined patterning with respect to several genes. Therefore, strategies to deal with multiple objectives need to be considered. In this case, the solution to the problem stated in Eq. (3) becomes the set:

$$\{x \in X \mid \nexists x' \in X : x' \leq x \wedge x \not\leq x'\}, \quad (5)$$

where x, x' are candidate solutions in the parameter space $X \subseteq \mathbb{R}^n$ and ' \leq ' denotes the weak Pareto-dominance relation with respect to the vector valued function $\mathbf{h}(x)$. For two vectors $x, x' \in \mathbb{R}^n$, x is said to weakly dominate x' ($x \leq x'$) with respect to $\mathbf{h}(x) = (h_1(x), \dots, h_m(x))$ iff $h_i(x) \leq h_i(x') \forall i \in \{1, \dots, m\}$. Thereby, Eq. (5) represents the set of all optimal solutions or Pareto-set of the multiobjective optimization problem.

Commonly, there are at least two different approaches to identify solutions in this set: (i) methods where all objective functions are aggregated into a single objective, and (ii) methods that consider all objectives simultaneously. With respect to the former approach, possible aggregations are weighted sum approaches or

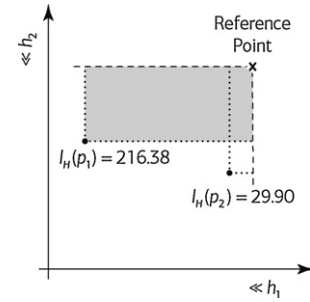


Fig. 5. Hypervolume indicator for a minimization problem with two objectives. The hypervolume for a point p in the objective space is defined by the volume of the hyper-cube spanned by the point and a reference point. The hypervolume spanned by the point p_1 is shown in gray. During selection, the hypervolume indicator values I_H can be used to build a ranking on different candidate vectors that is a total order and compliant with the concept of Pareto dominance.

scalarizations like Chebyshev scalarization (Miettinen, 1999). In the latter case multiple objectives are considered simultaneously by comparing different candidate solutions using indicators based on the concept of Pareto dominance (Deb, 2001).

In comparison, approaches explicitly considering all objectives simultaneously have the advantage that they can identify a set of solutions contained in the set defined by Eq. (5) while aggregation approaches tend to show less diversity. Although in principle a single fitting parameter setting might be enough to solve the task of model calibration, a set of settings can provide further information with respect to, e.g., robustness of the proposed model. In addition, for a range of different optimization tasks, studies have shown that considering multiobjective formulations can have a beneficial restructuring effect on the problem landscape, facilitating the optimization process (Brockhoff et al., 2007; Handl et al., 2008a,b; Neumann and Wegener, 2006).

Nevertheless, singleobjective approaches have the advantage that they impose a total order on the parameter space with respect to the optimization criterion which simplifies selection processes during optimization. Approaches based on the concept of Pareto dominance in turn only impose a partial order, introducing possible ambiguities during optimization. To resolve this matter, state of the art multiobjective approaches use refinements of the Pareto dominance resolving these ambiguities and establishing a total order, e.g., refinements like the hypervolume (Zitzler and Thiele, 1998; Zitzler et al., 2008, 2003). For hypervolume calculation, a reference point is introduced in the objective space and the quality of a given candidate solution is evaluated based on the volume enclosed by the hyper-cube spanned by a candidate solution and the reference point (see Fig. 5).

To gain flexibility in terms of numbers of considered objectives, there exists a multiobjective extension of the CMA-ES, the MO-CMA-ES (Igel et al., 2007): in each generation a set or population of CMA-ESs is used, with a population size of λ_{MO} . To generate a new population, each of the λ_{MO} CMA-ESs of the current population generates a single offspring. Instead of a selection just on the offspring, for each CMA-ES the selection is done on the old CMA-ES and its offspring. Thereby λ_{MO} offspring CMA-ES are generated and the population of CMA-ESs for the next generation is selected from the current population and the offspring generated thereof.

3.3. Combining optimization model and optimization method

The proposed optimization model is based on the idea that the parameter calibration process can be decomposed into a series of only partly depending optimization steps. An example calibration run for a one-dimensional SAM model is shown in Fig. 6. Using such a scheme results in the question how to determine when transitions

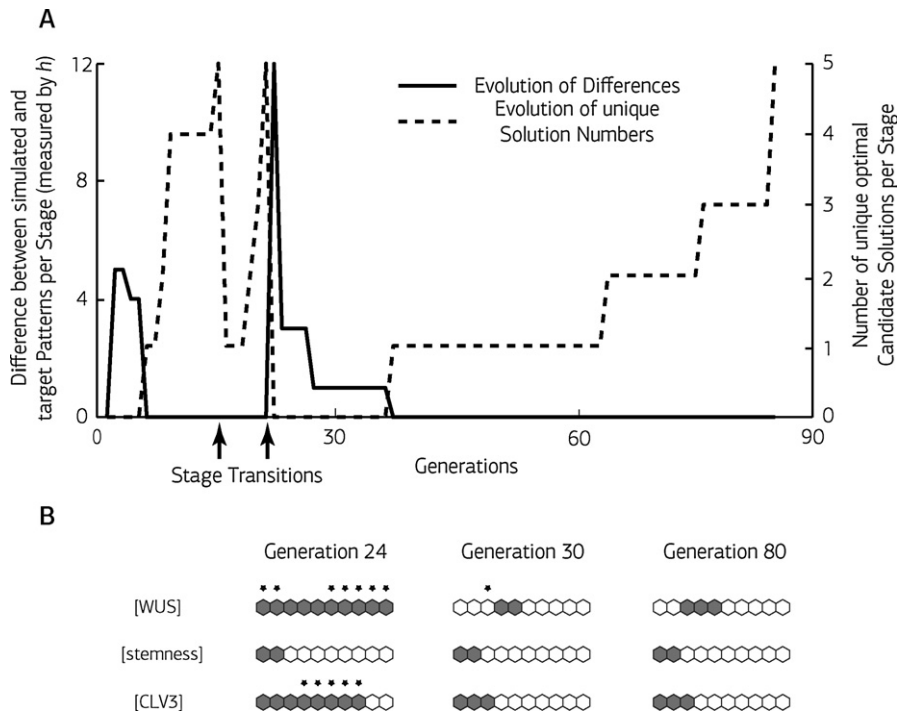


Fig. 6. Example calibration run for a one dimensional SAM model. (A) Evolution of the difference measure h during the different calibration stages for the best individual of each generation. Transitions between subsequent stages tend to result at least in a loss in the number of distinct candidate solutions that had been optimal during a previous stage, often accompanied by a loss in match between simulated patterns and target patterns for the respective stage. (B) Simulated patterns for different candidate solutions sampled during the third stage of the calibration process. Resulting patterns are shown for the three model entities [WUS], [stemness], and [CLV3]. Here, filled hexagons represent cells with a high level of expression of the respective model entity while empty hexagons show low expression. Hexagons marked with a star are cells where the simulated expression level deviates from the target level.

between different steps should occur. Further on, choosing to use the MO-CMA-ES for parameter calibration in the form it is described above, access to additional details on sample distributions resulting in good candidate solutions is provided. Thereby, a second question of how to preserve such information during different steps arises. In the following, these two issues are discussed and some remarks concerning a suitable representation of the search space in the MO-CMA-ES are given.

3.3.1. Stage transition

Since pretests showed that for a successful sequential optimization it is necessary that the stage change only occurs when a suitable diversity of sufficiently good parameter settings is accumulated for a given stage, stage changes occur once at least 50% of the λ_{MO} CMA-ES in the population of the MO-CMA-ES have identified a unique parameter setting with an optimal fitness of 0 for all considered criteria in the respective stage.¹ This results in two different stopping criteria for the algorithm as it is shown in Algorithm 4 in Igel et al. (2007):

1. The number of the allowed fitness evaluations is exceeded.
2. The population converges.

In case the algorithm converges in an early stage while fitness evaluations are left, it is restarted on the parameter space for the next stage using the respective objectives.

¹ In pretests we first compared variants where a stage transition occurs as soon as during a stage a single optimal candidate solution is found to a variant where transitions occur after at least 50% of the considered candidate solutions are optimal. Thereby, it turned out that these 50% most of the time had been copies of each other. We then extended the 50% requirement by further demanding that the candidate solutions need to represent unique parameter settings. During these tests, the influence of the exact percentage has not been further explored.

3.3.2. Transfer of information on sample distributions

As discussed above, it could be beneficial for the optimization process to transfer information on problem structure or dependencies of parameters between consecutive stages and the design of the MO-CMA-ES naturally supports such transfers: on top of a parameter setting representing the best guess of the heuristic for the considered optimization task, the user is provided with further information on the last search distribution N from which the final parameter setting was sampled. Thereby, the user gets a hand on information concerning dependencies and conditioning (reflected by the covariance matrix C) and overall scaling (stored in the scaling factor s) of the section of the parameter space containing promising solutions. While the CMA-ES typically is started using the identity matrix as starting covariance matrix C_{new} , in the described scenario it is possible to replace sub-matrices of C_{new} by entries taken from a covariance matrix generated for an earlier stage C_{prev} . In addition, information on scaling can be incorporated as well when comparing the scaling S_{prev} resulting from optimizing an earlier stage to the initial scaling S_{new} : using the quotient $(S_{prev}/S_{new})^2$ as a factor to scale entries taken from C_{prev} . In conclusion, for the re-initialization following a stage transition:

- either only the newly added parameters from the respective stage are considered and the search distributions for these parameters are initialized using the default identity matrices;
- or all parameters remain variable but still the new search distributions are initialized using the default;
- or the entries of the covariance matrices referring to parameters from earlier stages are transferred from the covariance matrices used during the last cycle of the previous stage;
- or on top of the covariance matrix entries, the scaling factors from the previous stage are transferred as well.

Table 1
Overview on computational approaches (top part) that are considered in two variants (bottom part).

<i>base</i>	Only the last stage of the developmental process is considered for model calibration.
<i>para</i>	All stages of the developmental process are considered in parallel for model calibration.
<i>fix</i>	All stages of the developmental process are considered for model calibration but in a sequential manner. Here, no information is transferred between the different phases of the calibration process and parameters already optimized during earlier stages are fixed.
<i>new</i>	All stages of the developmental process are considered for model calibration but in a sequential manner. Here, no information is transferred between the different phases of the calibration process and all considered parameters remain free.
<i>adapt – I</i>	Another sequential approach that transfers information on the last used covariance matrix <i>C</i> between phases with all considered parameters remaining free.
<i>adapt – II</i>	Another sequential approach that transfers information on the last used covariance matrix <i>C</i> and the scalings <i>s</i> between phases with all considered parameters remaining free
SO	Singleobjective variant where all difference functions <i>h</i> are aggregated to form a single objective value. They are aggregated using equal weights
MO	Multiobjective variant that in case of the baseline approach <i>base</i> and the sequential approaches considers all difference functions <i>h</i> of the respective stage simultaneously. In case of the parallel approach <i>para</i> , the difference functions of the stages are aggregated into one objective for each stage, resulting in three simultaneously considered objectives.

3.3.3. Search space representation

In addition to these details on optimization methodology, the question how the search space $X \subseteq \mathbb{R}^n$ is best represented in the optimization process should be addressed: while the MO-CMA-ES is designed to handle real-valued spaces, considered model parameters like reaction rates, basal expression terms, degradation rates, kinetic constants as well as diffusion constants tend to live in a logarithmic scale within certain intervals marking a feasible region. To facilitate handling parameters in the evolution strategy, the real-valued parameter space *X* is mapped to log-scale and normalized to [0, 1] before it is handed over to optimization. In case of the considered SAM model, the parameter space considered during optimization is $X = [0, 1]^{15}$ and only during the third stage the full dimensional parameter space needs to be considered: two of these fifteen parameters are exclusively used for the third stage. In the second stage, thirteen parameters are considered, with five of these newly introduced in comparison to the first stage; resulting in eight parameters used during the first stage.

4. Results and discussion

In the following, it is investigated how experimental data can be used in the process of model calibration or model parameter optimization. In this regard hypotheses are tested that the inclusion of information on intermediate system states can facilitate parameter optimization for GRN models in developmental biology for which mostly qualitative data is available. As example system the model for emergence and maintenance of the SAM in *A. thaliana* presented in Hohm et al. (2010) is used.

4.1. Test system

The developmental trajectory of the SAM can be hierarchically decomposed into three different stages with respect to time

1. Formation of a spatially confined domain of cells expressing the *WUS*, the so called OC.
2. Formation of a spatially confined domain of cells taking up stem cell identity, the SCD.
3. Relative spatially arrangement of the two functional domains.

For each stage there exists a target patterning with respect to the considered biological entities (see Fig. 3), the emergence of which is to be reproduced with the model. During the three stages the following difference functions are taken into account:

Stage 1: h_{WUS}^1 measuring the fit of a developing OC;

Stage 2: h_{WUS}^2 and h_{st}^2 measuring the fit of developing OC and SCD;

Stage 3: h_{WUS}^3 , h_{st}^3 , and h_{CLV3}^3 measuring the match of developing OC, SCD, and area under CLV3 influence.

4.2. Test setup

As already described, there is a range of possibilities to consider information on the developmental trajectory during model calibration: (i) a baseline approach using only the final system state during model calibration, (ii) an approach that simultaneously considers all three stages, (iii) approaches that consider the stages in a sequential manner. Here, the sequential approaches are differentiated by the amount of information that is transferred between the calibration process of subsequent stages:

- only those parameters newly introduced to the model in the respective stage are optimized and all previously calibrated parameters remain fixed (*fix*);
- approaches where in each stage all respective parameters are optimized but no information transfer takes place (*new*), approaches where between stages covariance matrices *C* of respective search distributions are transferred (*adapt-I*);
- approaches where between stages covariance matrices *C* and scaling factors *s* of respective search distributions are transferred (*adapt-II*).

Since in all these approaches a set of difference functions needs to be considered simultaneously at least during certain phases, two variants of each approach are considered: (i) a singleobjective variant where all difference functions are summed up to form an aggregated difference function, and (ii) a variant that considers all objectives simultaneously using a hypervolume based approach (see Fig. 5). A list of all approaches is given in Table 1.

The different strategies to include these information are tested using the MO-CMA-ES as method for parameter optimization with the parameter settings listed in Table 2. Possible gains are evaluated with respect to convergence of the optimization process and savings in necessary overall computation time for model simulations. Thereby, for the latter criterion one has to bear in mind that

Table 2
Parameter settings used for the MO-CMA-ES.

Parameter	Value
λ_{SO}	1
λ_{MO}	10
Allowed model simulations	3000
Convergence criterion	Accumulation of at least 5 distinct candidate solutions with optimal objective values

Table 3
Overview on computational costs for simulations of different stages. For each stage 50 simulations on the one dimensional 10 cell system for representative parameter settings have been done and their respective runtime in seconds have been recorded. Presented are the mean computation times and their respective standard deviations (*std*) per stage as well as per stage runtime normalized with the number of considered species.

	1st stage (2 genes)	2nd stage (4 genes)	3rd stage (5 genes)	1st stage, normalized	2nd stage, normalized	3rd stage, normalized
Mean in s	18.2266	36.5133	45.4424	9.1133	9.1283	9.0885
std in s	0.1539	0.5203	0.4352	0.0770	0.0130	0.0870

the computational cost during parameter estimation stems from simulation time while the optimization technique itself introduces only negligible computational overhead. Therefore, when for some model evaluations instead of the complete modeled system it is sufficient to simulate only a subsystem, this can result in considerable computational savings. In case of the considered SAM model, computational cost scales linearly with the number of simulated species (see Table 3)—thereby potentially providing significant savings when considering that parameter optimization runs on state of the art computers still run in the order of days.

Results for the different strategies are tested for statistical significance, first using the Kruskal–Wallis test (Conover, 1999) at a significance level of $\alpha = 0.05$. In these pairwise tests as H_0 hypothesis is tested if there is no significant difference in median with respect to:

convergence: capability to identify a parameter setting showing no difference between simulated pattern and target pattern

quality: aggregated score reached at the end of an optimization run,

runtime: used computation time for a run where a simulation for the first stage produces computational costs $c=0.4$, the second stage of $c=0.8$, and the third stage of $c=1$.

Thereafter, for all pairs of algorithms the differences are compared using the Conover–Inman procedure (Conover, 1999) with the same α level as in the Kruskal–Wallis test (see Table 4), resulting in a ranking of the strategies (see Table 5).

The testing is done on basis of 12 runs for each strategy, allowing up to 3000 simulations or 300 generations of the MO-CMA-ES using a population size of $\lambda_{mo} = 10$.

In addition, for this study we decided to circumvent some of the computation time necessary for simulations: instead of considering the two dimensional artificial longitudinal section through the SAM as spatial domain proposed in Hohm et al. (2010), it is restricted to a one dimensional system containing 10 cells (see Fig. 3).

Table 4
Pairwise comparison results between different strategies to include information on transient stages into the parameter optimization process: For each tested strategy, the pairwise significance test results are shown with respect to convergence (*c*), quality (*q*), and runtime (*r*). Thereby, the rows show entries in a column whenever the method depicted in a row shows significantly better performance with respect to one of the performance indicators. Significance testing is done using Kruskal–Wallis tests combined with the Conover–Inman procedure.

	<i>baseSO</i>	<i>baseMO</i>	<i>paraSO</i>	<i>paraMO</i>	<i>fixSO</i>	<i>fixMO</i>	<i>adapt – IISO</i>	<i>adapt – IIMO</i>	<i>adapt – ISO</i>	<i>adapt – IMO</i>	<i>newSO</i>	<i>newMO</i>
<i>baseSO</i>	---	---	---	---	---	---	---	---	---	---	---	---
<i>baseMO</i>	---	---	---	---	– q –	---	---	---	---	---	---	---
<i>paraSO</i>	---	c – –	---	– r	cq –	cq –	---	---	c – –	---	---	---
<i>paraMO</i>	---	---	---	---	– q –	---	---	---	---	---	---	---
<i>fixSO</i>	– r	– r	---	– r –	---	---	---	---	---	---	---	---
<i>fixMO</i>	– r	– r	---	– r –	---	---	---	---	---	---	---	---
<i>adapt – IISO</i>	– qr	– qr	– r	– qr	cqr	cqr	---	---	c – r	---	---	---
<i>adapt – IIMO</i>	– qr	cqr	– r	cqr	cqr	cqr	---	---	cqr	---	---	---
<i>adapt – ISO</i>	– r	– r	– r	– r	– q –	---	---	---	---	---	---	---
<i>adapt – IMO</i>	cqr	cqr	cqr	cqr	cqr	cqr	---	---	cqr	---	---	– q –
<i>newSO</i>	cqr	– r	– r	– r	cq –	cq –	---	---	---	---	---	---
<i>newIIMO</i>	cqr	– r	– r	– r	cq –	c – r	---	---	---	---	---	---

4.3. Comparison

With the comparison of the proposed approaches, the two hypotheses are validated that (i) inclusion of information on transient tissue patterning improves the overall convergence of model calibration processes and (ii) that exploiting such information is capable of reducing the necessary computation time.

4.3.1. Results: convergence properties

Addressing the first hypothesis, the baseline approaches *baseSO* and *baseMO* are compared to strategies where for every parameter setting that is considered during the calibration process all three stages are simulated, namely *paraSO* and *paraMO*. Indeed, inclusion of these information improves the convergence of the parameter optimization process significantly (see Table 4): *paraSO* shows better convergence properties than both, *baseSO* and *baseMO*. At the same time, *paraMO*, *baseSO*, and *baseMO* are indifferent with respect to convergence.

Including the sequential approaches into the comparison, convergence and quality properties are further improved: *adapt – IISO*, *adapt – IIMO*, and *adapt – IMO* show significant improvements compared to *baseSO*, *baseMO*, and *paraMO*. This finding probably has to be attributed to the fact that the dependence between the different stages during development can be exploited when information on successful search distributions for the parameter subspaces from previous stages is transferred to later stages. An idea that is supported by the fact that the strategies that do not transfer such information but always start off with a new search distribution (*newSO* and *newMO*) are not significantly better than either *paraSO* or *paraMO* (see Table 4). Although it is beneficial to transfer information on search distributions between stages, the early stages seem to be insufficient to already identify final settings for the involved parameters that remain fixed during later stages. Respective strategies *fixSO* and *fixMO* are both significantly worse than most of the approaches where parameters remain free.

Thereby, the results support the first hypothesis that inclusion of information on transient tissue patterning improves the overall convergence of model the calibration processes.

Table 5

Ranking on significance results of the different strategies to include information on transient stages into the parameter optimization process. For each of the tested strategies and all three performance indicators, convergence (*c*), quality (*q*), and runtime (*r*), the number of strategies significantly besting the respective strategy (–) as well as the number of strategies significantly bested by the respective strategy (+) are given as pair ‘–/+’.

	<i>baseSO</i>	<i>baseMO</i>	<i>paraSO</i>	<i>paraMO</i>	<i>FixSO</i>	<i>FixMO</i>	<i>adapt – IISO</i>	<i>adapt – IIMO</i>	<i>adapt – ISO</i>	<i>adapt – IMO</i>	<i>newSO</i>	<i>newMO</i>
<i>c</i>	6/0	3/0	0/5	2/0	6/0	6/0	0/4	0/6	4/0	0/8	1/3	1/3
<i>q</i>	6/0	3/1	0/3	3/1	9/0	5/0	0/5	0/6	2/1	0/7	0/5	1/2
<i>r</i>	8/0	8/0	6/1	9/0	3/3	4/0	0/7	0/7	3/4	0/7	0/4	0/5

4.3.2. Results: computational cost

With respect to the second hypothesis that exploitation of information on transient tissue patterning is capable of reducing the necessary computation time, again first the baseline approaches *baseSO* and *baseMO* are compared to the parallel approaches *paraSO* and *paraMO*. While the parallel approaches have access to a maximum of information, simulating always every stage introduces considerable additional computational cost. In case of the SAM model where for the first stage two species, for the second stage four species, and for the final stage 5 species are considered, this amount to 2.2 times the computational effort.

Nevertheless, in terms of runtime the four strategies are indistinguishable despite the extra in computational cost (see Table 4). This can be explained by the slightly better convergence properties of the latter two approaches (even when not significant in case of *paraMO*): some of the runs converge already quite fast using much less computation time than the baseline approaches.

Considering the sequential approaches as well, all of these provide a significant improvement in necessary computation time when compared to *baseSO*, *baseMO*, *paraSO*, and *paraMO* (see Table 4). Thereby, the second hypothesis is validated.

Only the influence of using multiobjective variants compared to singleobjective variants is less clear: apart from the variants where all stages are considered simultaneously, the multiobjective approaches are superior to the singleobjective ones (see Table 5). Since a pre-study has shown that diversity in the found parameter setting is crucial for a successful optimization process, this can be explained with the fact that multiobjective approaches in general support diversity while even set based singleobjective approaches tend to show less diversity. Still, in case of *para* and *new*, the singleobjective variants seem to be superior. A possible explanation for this finding might be that in these cases the multiobjective approach in combination with discrete fitness functions introduce ambiguities that can not be resolved using the hypervolume and in consequence obscure the optimization process.

5. Conclusions

In this study we addressed the problem of model calibration for differential equation models in the area of developmental biology. In this domain, researchers are interested in understanding the emergence of patterns with respect to gene expression profiles in considered tissues. The calibration of such time and space dependent models is difficult due to the usually non-linear dependences between model entities as well as due to the fact that it is difficult to acquire high-resolution quantitative data concerning these systems; instead, usually only qualitative data is available.

To aid the process of model calibration we therefore proposed a method to increase the degree of utilization of domain knowledge: instead of only considering the final system state of the developmental trajectory during calibration, a scheme is designed that in addition allows to include information on transient system states. Using a model for stem cell homeostasis in *A. thaliana* as test system, it turned out that the enhanced use of the available data boosts the success rate of the calibration process. Especially, considering the different transient states in a sequential manner during the

calibration process not only positively influences the convergence rate but has a beneficial impact on the necessary computation time by allowing to consider only subsystems during early stages and providing synergies between the different stages.

The proposed approach thereby makes use of a hierarchical decomposition of both, the developmental trajectory and the underlying regulative system. In difference to other hierarchical approaches, not just in the field of computational biology but as well in most engineering applications, here the decomposition of the target system is not supposed to happen in an automated way but is explicitly designed to provide a convenient way to include usually available domain knowledge in the calibration process. Such an approach is especially well suited for developmental systems since they are inherently hierarchically structured and knowledge on both, the developmental trajectory and involved system components is commonly available.

Still, a similar approach provides a promising route to tackle optimizations tasks in different areas, e.g., engineering design: alike developmental systems, systems designed by humans tend to consist of modules the interactions between which are known but due to their often non-linear nature hard to predict. Thereby, such systems provide a starting position comparable to the one found in developmental systems.

Acknowledgements

The authors would like to thank Ralf Müller and Rüdiger Simon for providing the in situ hybridization images shown in Fig. 1.

Appendix A. Models for different stages and details for numerical simulations

For the approach to model calibration including information on the developmental trajectory of the respective system, the model for stem cell homeostasis in the SAM of *A. thaliana* presented in Hohm et al. (2010) is decomposed into models for different stages of its development. Before the newly introduced models for earlier developmental stages are presented, first the full model is repeated:

$$\frac{\partial[WUS]}{\partial t} = D_s \Delta[WUS] + \xi \rho_{anc} \frac{[WUS]^2 [facX]}{1 + [CLV3]^3} - \mu_{WUS} [WUS] + \sigma_{WUS}, \quad (A.1)$$

$$\frac{\partial[facX]}{\partial t} = D_q \Delta[facX] - \xi \rho_{anc} \frac{[WUS]^2 [facX]}{1 + [CLV3]^3} + \frac{\sigma_{facX}}{1 + [facX]/K_{facX}}, \quad (A.2)$$

$$\frac{\partial[WUS_{sig}]}{\partial t} = D_q \Delta[WUS_{sig}] + \rho_{WUS_{sig}} [WUS] - \mu_{WUS_{sig}} [WUS_{sig}], \quad (A.3)$$

$$\frac{\partial[st]}{\partial t} = D_s \Delta[st] + 1_{id(i)} \rho_{st} \frac{[WUS_{sig}]/K_{st}}{1 + ([WUS_{sig}]/K_{st})^5} - \mu_{st} [st], \quad (A.4)$$

$$\frac{\partial[CLV3]}{\partial t} = D_q \Delta[CLV3] + \rho_{CLV3} [st] - \mu_{CLV3} [CLV3]. \quad (A.5)$$

Table A.1
Feasibility ranges used for different model parameters during optimization.

Parameter	Range				
	D	ρ	μ	σ	K
Range	[0.0001, 0.5]	[0.01, 1.5]	[0.0001, 0.1]	[0.0001, 0.01]	[0.001, 1]

Here, the D_q and D_s are diffusion constants which are assumed to be similar for the quickly diffusing components ($[facX]$, $[WUS_{sig}]$, and $[CLV3]$) and for the local components ($[WUS]$ and $[st]$) that still undergo some weak leakage diffusion. The ρ_i with $i \in \{anc, WUS_{sig}, st, CLV3\}$ are reaction rates that are equal in all cells with one exception being ρ_{anc} , the so called anchoring distribution that is necessary in the model to compensate for missing structural information guiding exact positioning of the functional domains active in the meristem. μ_i with $i \in \{WUS, WUS_{sig}, st, CLV3\}$ are degradation rates, σ_{WUS} and σ_{facX} are terms representing basal expression, $\mathbf{1}_{id}$ is a characteristic function determining stem cell competent layers, and $\xi \in [-0.025, 0.025]$ is a random perturbation necessary to initiate pattern formation. An overview on feasibility intervals used for the different types of parameters is given in Table A.1.

$$\mathbf{1}_{id}(i) = \begin{cases} 1, & \text{if cell } i \in \{L1, L2\} \\ 0, & \text{else} \end{cases} \quad (\text{A.6})$$

During the first stage of SAM development, only the so called OC is formed. To initiate this domain of WUS expressing cells only the model entities $[WUS]$ and $[facX]$ need to be considered resulting in a reduced model given by the following equations:

$$\frac{\partial[WUS]}{\partial t} = D_s \Delta[WUS] + \xi \rho_{anc}[WUS]^2[facX] - \mu_{WUS}[WUS] + \sigma_{WUS}, \quad (\text{A.7})$$

$$\frac{\partial[facX]}{\partial t} = D_q \Delta[facX] - \xi \rho_{anc}[WUS]^2[facX] + \frac{\sigma_{facX}}{1 + [facX]/K_{facX}}. \quad (\text{A.8})$$

Moving on to the second developmental stage, the model of stage one is extended by components modeling the formation of a SCD, yet leaving out the feedback from SCD to the OC. The model for stage two is given by the following equations:

Moving on to the second developmental stage, the model of stage one is extended by components modeling the formation of a SCD, yet leaving out the feedback from SCD to the OC. The model for stage two is given by the following equations:

$$\frac{\partial[WUS]}{\partial t} = D_s \Delta[WUS] + \xi \rho_{anc}[WUS]^2[facX] - \mu_{WUS}[WUS] + \sigma_{WUS}, \quad (\text{A.9})$$

$$\frac{\partial[facX]}{\partial t} = D_q \Delta[facX] - \xi \rho_{anc}[WUS]^2[facX] + \frac{\sigma_{facX}}{1 + [facX]/K_{facX}}, \quad (\text{A.10})$$

$$\frac{\partial[WUS_{sig}]}{\partial t} = D_q \Delta[WUS_{sig}] + \rho_{WUS_{sig}}[WUS] - \mu_{WUS_{sig}}[WUS_{sig}], \quad (\text{A.11})$$

$$\frac{\partial[st]}{\partial t} = D_s \Delta[st] + \mathbf{1}_{id}(i)\rho_{st} \frac{([WUS_{sig}]/K_{st})^5}{1 + ([WUS_{sig}]/K_{st})^5} - \mu_{st}[st]. \quad (\text{A.12})$$

The SAM simulations are done using numerical integration of the respective systems. For the integration an implicit/explicit scheme based on a modified Crank-Nicolson integrator combined with an Adams-Bashford scheme (Ruuth, 1995) is used. As spatial discretization for the Crank-Nicolson scheme a grid of cellular resolution is used and time is discretized using a constant time

steps $\delta_t = 0.5$ of dimensionless time. Each simulation encompasses 120,000 time steps.

References

Amonlirdviman, K., Khare, N.A., Tree, D.R., Chen, W.S., Axelrod, J.D., Tomlin, C.J., 2005. Mathematical modeling of planar cell polarity to understand domineering nonautonomy. *Science* 307 (5708), 423–426.

Auger, A., Hansen, N., 2005. Performance evaluation of an advanced local search evolutionary algorithm. In: Congress on Evolutionary Computation (CEC 2005), vol. 2. IEEE Press, Piscataway, NJ, USA, pp. 1777–1784.

Bleckmann, A., Simon, R., 2009. Interdomain signaling in stem cell maintenance of plant shoot meristems. *Mol. Cells* 27 (6), 615–620.

Bouyer, D., Geier, F., Kragler, F., Schnittger, A., Pesch, M., Wester, K., Balkunde, R., Timmer, J., Fleck, C., Hülskamp, M., 2008. Two-dimensional patterning by a trapping/depletion mechanism: the role of TTG1 and GL3 in *Arabidopsis trichome* formation. *PLoS Biol.* 6 (6), e141.

Brand, U., Feltscher, J.C., Hobe, M., Meyerowitz, E.M., Simon, R., 2000. Dependence of stem cell fate in *Arabidopsis* on a feedback loop regulated by CLV3 activity. *Science* 289 (5479), 617–619.

Brockhoff, D., Friedrich, T., Hebbinghaus, N., Klein, C., Neumann, F., Zitzler, E., 2007. Do additional objectives make a problem harder? In: Thierens, D., et al. (Eds.), Genetic and Evolutionary Computation Conference (GECCO 2007). ACM Press, New York, NY, USA, pp. 765–772.

Clark, S.E., Williams, R.W., Meyerowitz, E.M., 1997. The CLAVATA1 gene encodes a putative receptor kinase that controls shoot and floral meristem size in *Arabidopsis*. *Cell* 89 (4), 575–585.

Conover, W.J., 1999. Practical Nonparametric Statistics, 3rd edition. John Wiley, Chichester, UK.

Deb, K., 2001. Multi-Objective Optimization Using Evolutionary Algorithms. Wiley, Chichester, UK.

Fletcher, J.C., Brand, U., Running, M.P., Simon, R., Meyerowitz, E.M., 1999. Signaling of cell fate decisions by CLAVATA3 in *Arabidopsis* shoot meristems. *Science* 283 (5409), 1911–1914.

Foster, J.A., 2001. Evolutionary computation. *Nat. Rev. Genet.* 2 (6), 428–436.

Geier, F., Lohmann, J.U., Gerstung, M., Maier, A.T., Timmer, J., Fleck, C., 2008. A quantitative and dynamic model for plant cell regulation. *PLoS ONE* 3 (10), e3553.

Gordon, S.P., Heisler, M.G., Reddy, G.V., Ohno, C., Meyerowitz, E.M., 2007. Pattern formation during de novo assembly of the *Arabidopsis* shoot meristem. *Development* 134 (19), 3539–3548.

Groß-Hardt, R., Lenhard, M., Laux, T., 2002. WUSCHEL signaling functions in inter-regional communication during *Arabidopsis* ovule development. *Gene Dev.* 16 (21), 1129–1138.

Handl, J., Lovell, S., Knowles, J., 2008a. Multiobjectivization by decomposition of scalar cost functions. In: Rudolph, G., et al. (Eds.), Conference on Parallel Problem Solving From Nature (PPSN X), vol. 5199 of LNCS. Springer, pp. 31–40.

Handl, J., Lovell, S.C., Knowles, J., 2008b. Investigations into the effect of multiobjectivization in protein structure prediction. In: Rudolph, G., et al. (Eds.), Conference on Parallel Problem Solving From Nature (PPSN X), vol. 5199 of LNCS. Springer, pp. 702–711.

Hansen, N., Ostermeier, A., 2001. Completely derandomized self-adaptation in evolutionary strategies. *Evol. Comput.* 9 (2), 159–195.

Hohm, T., Zitzler, E., 2007. Modeling the shoot apical meristem in *A. thaliana*: parameter estimation for spatial pattern formation. In: Marchiori, E., Moore, J.H., Rajapakse, J.C. (Eds.), Evolutionary Computation, Machine Learning and Data Mining in Bioinformatics (evoBIO 2007), vol. 4447 of LNCS. Springer, pp. 102–113.

Hohm, T., Zitzler, E., 2009a. A multiobjective evolutionary algorithm for numerical parameter space characterization of reaction diffusion systems. In: Kadiramanathan, V., et al. (Eds.), International Conference on Pattern Recognition in Bioinformatics (PRIB 2009), vol. 5780 of LNBI. Springer, Heidelberg, Germany, pp. 162–174.

Hohm, T., Zitzler, E., 2009b. Multicellular pattern formation: parameter estimation for ODE-based gene regulatory network models. *IEEE Eng. Med. Biol.* 28 (4), 52–57.

Hohm, T., Zitzler, E., 2009c. Multiobjectivization for parameter estimation: a case-study on the segment polarity network of *Drosophila*. In: Rothlauf, F., et al. (Eds.), GECCO 09: Genetic and Evolutionary Computation Conference (GECCO 2009). ACM, New York, NY, USA, pp. 209–216.

Hohm, T., Zitzler, E., Simon, R., 2010. A dynamic model for stem cell homeostasis and patterning in *Arabidopsis* meristems. *PLoS ONE* 5 (2), e9189.

Horst, R., Pardalos, P.M., Van Thoai, N., 1995. Introduction to Global Optimization, 1st edition. Springer, Berlin, Germany.

Igel, C., Hansen, N., Roth, S., 2007. Covariance matrix adaptation for multi-objective optimization. *Evol. Comput.* 15 (1), 1–28.

Jeong, S., Trotochaud, A.E., Clark, S.E., 1999. The *Arabidopsis* CLAVATA2 gene encodes a receptor-like protein required for the stability of the CLAVATA1 receptor-like kinase. *Plant Cell* 11 (10), 1925–1934.

Jönsson, H., Heisler, M., Reddy, G.V., Agrawal, V., Gor, V., Shapiro, B.E., Meyerowitz, E.M., 2005. Modeling the organization of the WUSCHEL expression domain in the shoot apical meristem. *Bioinformatics* 21 (Suppl. 1), i232–i240.

Koch, A.J., Meinhardt, H., 1994. Biological pattern formation: from basic mechanisms to complex structures. *Rev. Mod. Phys.* 66 (4), 1481–1510.

Kondo, T., Sawa, S., Kinoshita, A., Mizuno, S., Kakimoto, T., Fukuda, H., Sakagami, Y., 2006. A plant peptide encoded by CLV3 identified by in situ MALDI-TOF MS analysis. *Science* 313 (5788), 845–848.

- Laux, T., Mayer, K.F.X., Berger, J., Jürgens, G., 1996. The WUSCHEL gene is required for shoot and floral meristem integrity in Arabidopsis. *Development* 122 (1), 87–96.
- Leibfried, A., To, J.P.C., Busch, W., Stehling, S., Kehle, A., Demar, M., Kieber, J.J., Lohmann, J.U., 2005. WUSCHEL controls meristem function by direct regulation of cytokinin-inducible response regulators. *Nature* 438 (7071), 1172–1175.
- Mayer, K.F.X., Schoof, H., Haecker, A., Lenhard, M., Jürgens, G., Laux, T., 1998. Role of WUSCHEL in regulating stem cell fate in the Arabidopsis shoot meristem. *Cell* 95 (6), 805–815.
- Mendes, P., Kell, D.B., 1998. Non-linear optimization of biochemical pathways: applications to metabolic engineering and parameter estimation. *Bioinformatics* 14 (10), 869–883.
- Miettinen, K., 1999. *Nonlinear Multiobjective Optimization*. Kluwer, Boston, MA, USA.
- Migdalas, A., Pardalos, P.M., Värbrand, P., 1997. *Multilevel Optimization: Algorithms and Applications*, 1st edition. Springer, Berlin, Germany.
- Mjolsness, E., Sharp, D.H., Reinitz, J., 1991. Connectionist model of development. *J. Theor. Biol.* 152 (4), 429–453.
- Moles, C.G., Mendes, P., Banga, J.R., 2003. Parameter estimation in biochemical pathways: a comparison of global optimization methods. *Genome Res.* 13 (11), 2467–2474.
- Müller, R., Bleckmann, A., Simon, R., 2008. The receptor kinase CORYNE of Arabidopsis transmits the stem cell-limiting signal CLAVATA3 independently of CLAVATA1. *Plant Cell* 20 (4), 934–946.
- Müller, R., Borghi, L., Kwiatkowska, D., Laufs, P., Simon, R., 2006. Dynamic and compensatory responses of Arabidopsis shoot and floral meristems to CLV3 signaling. *Plant Cell* 18 (5), 1188–1198.
- Murray, J.D., 2003. *Mathematical Biology*, vol. 2. Springer, New York, NY, USA.
- Nakamasu, A., Takahashi, G., Kanabe, A., Kondo, S., 2009. Interactions between zebrafish pigment cells responsible for the generation of Turing patterns. *Proc. Natl. Acad. Sci. U.S.A.* 106 (21), 8429–8434.
- Neumann, F., Wegener, I., 2006. Minimum spanning trees made easier via multi-objective optimization. *Natural Computing* 5(3), 305–319; conference version in Beyer et al. (Eds.), *Genetic and Evolutionary Computation Conference – GECCO 2005*, vol. 1. ACM Press, New York, USA, pp. 763–770.
- Ogawa, M., Shinohara, H., Sakagami, Y., Matsubayashi, Y., 2008. Arabidopsis CLV3 peptide directly binds CLV1 ectodomain. *Science* 319 (5861), 294.
- Quast, R., Baade, R., Reimers, D., 2005. Evolution strategies applied to the problem of line profile decomposition in QSO spectra. *Astron. Astrophys.* 431 (3), 1167–1175.
- Raffard, R., Amonlirdviman, K., Axelrod, J.D., Tomlin, C.J., 2006. Automatic parameter identification via the adjoint method, with application to understanding planar cell polarity. In: *IEEE Conference on Decision and Control (CDC 2006)*. IEEE Press, Piscataway, NJ, USA, pp. 13–18.
- Reinhardt, D., Frenz, M., Mandel, T., Kuhlemeier, C., 2003. Microsurgical and laser ablation analysis of interactions between the zones and layers of the tomato shoot apical meristem. *Development* 130 (17), 4073–4083.
- Ruuth, S.J., 1995. Implicit-explicit methods for reaction-diffusion problems in pattern formation. *J. Math. Biol.* 34 (2), 148–176.
- Savageau, M.A., 1979. Allometric morphogenesis of complex systems: derivation of the basic equations from first principles. *Proc. Natl. Acad. Sci. U.S.A.* 76 (12), 6023–6025.
- Stahl, Y., Simon, R., 2005. Plant stem cell niches. *Int. J. Dev. Biol.* 49 (5–6), 479–489.
- Strogatz, S.H., 2000. *Nonlinear Dynamics and Chaos. Studie in Nonlinearity*. Westview, Cambridge, MA, USA.
- Voit, E.O., 2000. *Computational Analysis of Biochemical Systems*. Cambridge University Press, Cambridge, UK.
- von Dassow, G., Meir, E., Munro, E.M., Odell, G.M., 2000. The segment polarity network is a robust developmental module. *Nature* 406 (6792), 188–192.
- Yamaguchi, M., Yoshimoto, E., Kondo, S., 2007. Pattern regulation in the stripe of zebrafish suggests an underlying dynamic and autonomous mechanism. *Proc. Natl. Acad. Sci. U.S.A.* 104 (12), 4790–4793.
- Zitzler, E., Thiele, L., 1998. Multiobjective optimization using evolutionary algorithms – a comparative case study. In: *Conference on Parallel Problem Solving from Nature (PPSN V)*, Amsterdam, pp. 292–301.
- Zitzler, E., Thiele, L., Bader, J., 2008. SPAM: set preference algorithm for multiobjective optimization. In: Rudolph, G., et al. (Eds.), *Conference on Parallel Problem Solving From Nature (PPSN X)*, vol. 5199 of LNCS. Springer, pp. 847–858.
- Zitzler, E., Thiele, L., Laumanns, M., Fonseca, C.M., Grunert da Fonseca, V., 2003. Performance assessment of multiobjective optimizers: an analysis and review. *IEEE Trans. Evol. Comput.* 7 (2), 117–132.